

Reflex optical sensor based on dual metal gratings with high angular sensitivity

Ji Xu (许吉)^{1*}, Chen Cheng (程晨)¹, Qiang Bai (白强)¹,
Jing Chen (陈璟)^{2,3}, and Jianping Ding (丁剑平)¹

¹Nanjing National Laboratory of Microstructures and School of Physics, Nanjing University, Nanjing 210093, China

²School of Physics and Key Laboratory of Weak Light Nonlinear Photonics, Nankai University, Tianjin 300071, China

³State Key Laboratory of Functional Materials for Informatics, Shanghai Institute of Microsystem and Information Technology, Chinese Academy of Sciences, Shanghai 200050, China

*Corresponding author: xuji@nju.edu.cn

Received November 17, 2010; accepted January 3, 2011; posted online April 28, 2011

An interesting reflection phenomenon in a dual metal grating (DMG) structure is studied, which is related to the competition between Fabry-Pérot (F-P) resonance effect and evanescent-field coupling effect inside the gap between the two composing single metal gratings. This competition leads to high angular sensitivity in response to the refractive index variation of the sample solution in the gap. A reflex optical sensor with high sensitivity based on DMG for detecting the change in refractive index is proposed and its performance theoretically is discussed.

OCIS codes: 050.2770, 260.2110, 280.4788.

doi: 10.3788/COL201109.060501.

Surface plasmon polariton (SPP) resonance is very sensitive to the change in refractive index near the interface. SPP resonance (SPPR) has been widely used in optical sensing technology and in many other applications such as in the pharmaceutical industry, water safety testing, and medical diagnostics^[1–3]. For the sensing technology, sensitivity is quite an important parameter for evaluating its performance^[1], which is the magnitude of the change in signal in response to the refractive index variation. Prism-coupling^[4] and grating-coupling techniques are mainly used to realize the excitation of SPP. Despite the high sensitivity of SPPR-based sensor with prism-coupling Kretschmann configuration, it is difficult to integrate the structure into an optical circuit because of its relatively big size. Grating-coupling SPPR-based sensor is relatively convenient for the excitation of SPP and for integration, but its sensitivity is slightly low^[2,5,6]. Over the last decade, novel microstructures such as dielectric-metal multilayers^[7,8] with prism-coupling configuration utilizing long-range SPP^[9], gratings^[10–12] and nanoparticle arrays^[13–15] supporting localized SPP, which can be easily integrated into optical circuits^[16], and some other configurations^[17,18] have been proposed to achieve higher sensitivity. Most of these schemes depend on the excitation of SPP at metal-dielectric (either smooth or structured) interfaces for sensing purpose.

In this letter, we propose a new kind of reflex optical sensor with high sensitivity based on the dual-metal grating (DMG) structure composed of two identical single metal gratings (SMGs) with subwavelength slit arrays^[19–21]. This DMG structure has many attractive properties. The Fabry-Pérot(F-P)-like resonance of coupled-SPP mode^[20] inside the slits can be considered as an intrinsic electromagnetic (EM) feature of the SMG structures, which is associated with enhanced local EM field and results in extraordinary EM transmission^[22,23]. In the DMG structures, two kinds of interactions be-

tween the two SMGs affect the EM transmission and reflection properties. We reveal the underlying physics of the displayed anti-crossing phenomenon in the reflection spectrum due to the competition between the two kinds of effects. A simple structure of optical sensor based on DMG is proposed, and its sensing performances are simulated and discussed. The simulation algorithm used here is the transfer matrix method proposed in Ref. [24].

When the wavelength is larger than the period of SMG, the non-zeroth-order diffracted waves are all evanescent, whereas the zeroth order is always propagating. Thus, in the DMG structure, when the gap G between the two SMGs is small enough, the evanescent-field coupling effect may dominate the interaction between the two SMGs and split peaks appear in the transmission spectrum^[19–21]. When the gap is big enough, the F-P resonance effect dominates the interaction. We focus on the situation when the two SMGs are neither too close nor too far away, thus both effects are comparable, leading to an effective competition between them. To reveal the unique feature of this competition, we calculate the reflection spectra for the true DMG structure when G varies from 500 to 1,500 nm under normal incidence (Fig. 1(a)) and for its simplified model with a trilayer structure based on the effective medium model^[19,20,25] (Fig. 1(b)). The effective medium model helps us distinguish the phenomena caused by the evanescent-field coupling effect^[20]. We use the same geometric parameters as those in Ref. [20], with the period of $d=1,000$ nm, the slit width of $a=100$ nm, and the thickness of $h=500$ nm for SMG. The metal is silver (Ag), which obeys the lossless Drude dispersion, and the two SMGs are aligned without lateral shift. For the effective medium model, the thickness and the refractive index of the slab are 77.5 nm and 10, respectively^[20]. The upper limit of the reflectance is set to be 5% to display the reflection minimum clearly. In Fig. 1(b), two straight reflection-

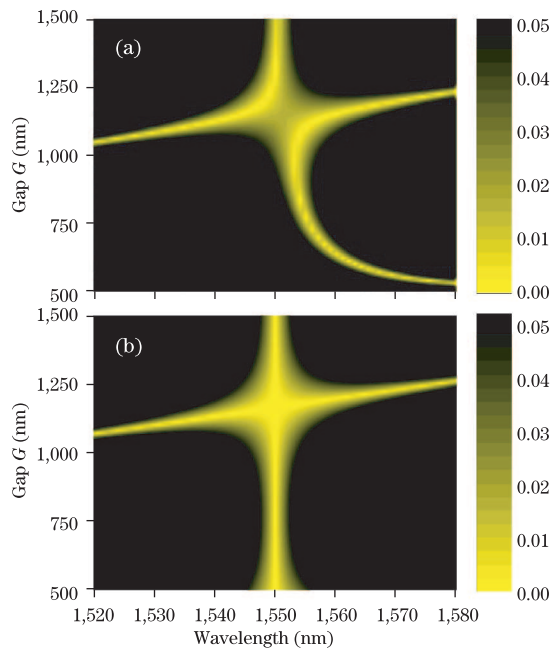


Fig. 1. Reflection spectra around the wavelength of 1,550 nm under normal incidence, with gap G ranging from 500 to 1,500 nm, $d=1,000$ nm, $a=100$ nm, and $h=500$ nm for SMG. (a) True DMG structure; (b) simplified structure by the effective medium model.

minimum lines intersect each other. The vertical straight line at 1,550 nm originates from the cascaded transmission through the two SMGs, while the slightly acclivitous straight line is caused by the F-P resonance effect. Compared with Fig. 1(b), there are two evident features in Fig. 1(a). First, the two intersecting lines split into two separated curves, exhibiting an obvious clear anti-crossing phenomenon. Second, the reflection-minimum curve is strongly bent when $G < 1,000$ nm. We can conclude that the evanescent-field coupling effect plays an important role in the two features; this means that the two features are caused by the coexistence or competition of the two effects.

We now investigate the dependency of reflectance on both incident angle θ and gap G at various wavelengths. The simulation results are shown in Fig. 2 at wavelengths of 1,560, 1,550, and 1,500 nm. The reflection-minimum curves can be classified into three kinds. Curve A is almost independent of the incident angle θ , and the gap difference between the two adjacent curves A is equal to a half wavelength. Hence, curve A is related to the F-P resonance in the gap. Curve B is not influenced by the gap G ; it depends strongly on the wavelength and is always located at a constant incident angle, implying that curve B is associated with the cascaded transmission through the two SMGs. Curve C depends strongly on both wavelength and incident angle and is related to the evanescent-field coupling effect. These three kinds of curves (A, B, and C) form an anti-crossing gap in the regime enclosed by the ellipse in Fig. 2. Curve C and the anti-crossing gap can be observed only when the wavelength is longer than the resonant wavelength of the coupled-SPP guided mode inside the slit, as shown in Figs. 2(a) and (b).

In general, high sensitivity is necessary in designing a

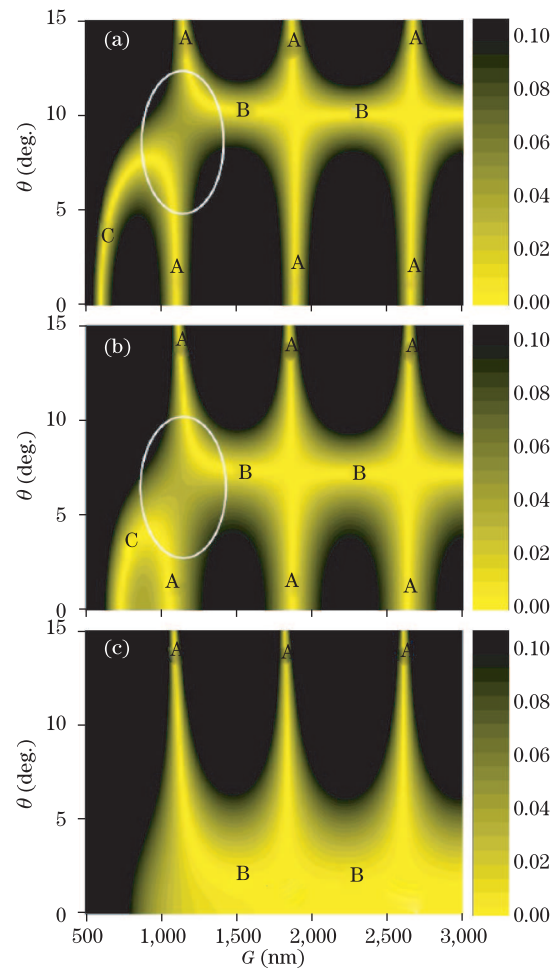


Fig. 2. Dependency of the reflectance on both incident angle θ and gap G at wavelengths of (a) 1,560, (b) 1,555, and (c) 1,550 nm, respectively.

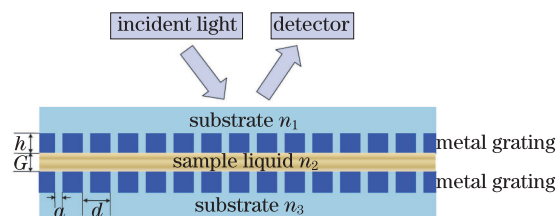


Fig. 3. Scheme of the reflex optical sensor based on DMG structure.

sensor. This is because the gap G is difficult to control in nanoscale, and curves B and C are sensitive to the incident angle θ . In addition, in practice, it is more convenient to collect the reflected signal under oblique incidence. Thus, in the simulation, we fix the gap G and seek for the reflection-minimum point by changing the incident angle θ . We now discuss the sensitivity of the different curves mentioned previously based on a designed optical sensor in the DMG configuration (Fig. 3). Two SMGs manufactured on a dielectric substrate are vertically aligned, and the target liquid flows into the gap between the two SMGs. The slits of the SMGs are filled with the same material as the substrate. A laser provides the incident light with p-polarization, and a detector records the reflection data. By measuring the incident

angle for reflection minimum, the change in refractive index on the sample liquid can be detected. For example, we first consider the SMG with the following parameters: $d=400$ nm, $a=50$ nm, and $h=140$ nm. The metal is Ag, which obeys the lossless Drude dispersion model, and the refractive indices of the dielectrics are $n_1=n_3=1.38$ (e.g., MgF_2)^[8] and $n_2=1.33$ (water). The corresponding wavelength λ_g of the reflection minimum (high transmission) caused by the coupled-SPP guided-mode resonance in SMG is 762 nm under normal incidence.

To evaluate the angular sensitivity of the sensor, we choose different values of n_2 . Figure 4 shows the dependency of the reflectance on both incident angle θ and gap G at a wavelength of 770 nm, with $n_2=1.330$ and 1.335, respectively. When n_2 is changed from 1.330 to 1.335 ($\Delta n_2=0.005$), the reflection behavior exhibits significant differences, implying that this DMG structure is a good candidate for the optical sensor. Appropriate values of λ and G should be chosen to enable the sensor to achieve optimal performance. Similar to Fig. 2, the reflection-minimum curves in Fig. 4 are classified into three categories: curves A, B, and C. To investigate the sensitivity, we choose three typical reflection-minimum points, as shown by the circles and arrows in Fig. 4. The first is located at the smaller gap regime on curve C with $G=280$ nm, the second is in the critical position on curve C with $G=340$ nm, and the third is in curve B with $G=550$ nm.

Figure 5(a) shows the dependency of the reflectance on θ at the wavelength of 770 nm (which is longer than λ_g) for $G=280$, 340, and 550 nm and for different values of $n_2=1.330$, 1.332, and 1.335. For a given G , as n_2 increases, the incident angle for reflection minimum decreases. We estimate the average sensitivity $S = \Delta\theta/\Delta n_2$, which are $S_{G=280}=338^\circ/\text{RIU}$, $S_{G=340}=220^\circ/\text{RIU}$, and $S_{G=550}=124^\circ/\text{RIU}$, where RIU is refractive index unit. This suggests that the sensitivity

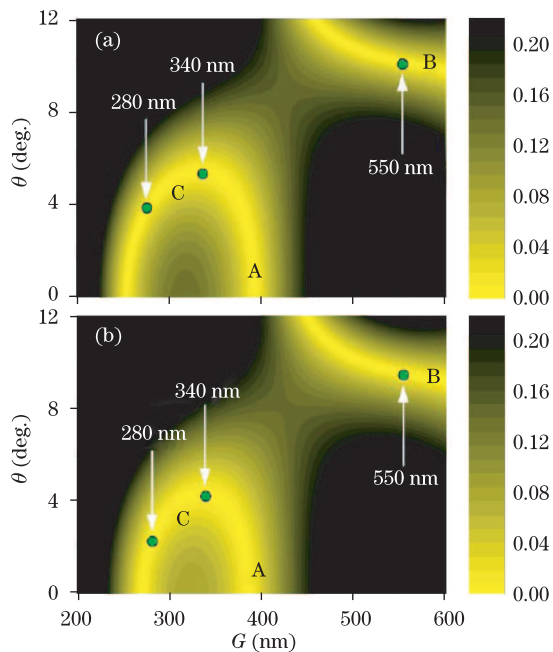


Fig. 4. Dependency of the reflectance on both incident angle θ and gap G at the wavelength of 770 nm for two different refractive indices of (a) 1.330 and (b) 1.335.

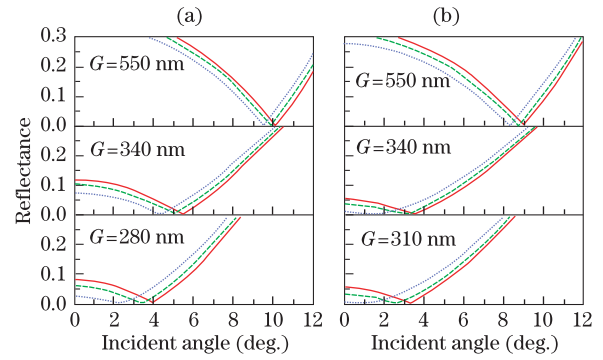


Fig. 5. Angular reflection spectra for three different refractive indices of 1.330, 1.332, and 1.335. (a) At the wavelength of 770 nm for three different gaps of 550, 340, and 280 nm; (b) at the wavelength of 768 nm for three different gaps of 550, 340, and 310 nm.

of curve C is higher than that of curve B, and that the sensitivity at the smaller gap G is higher than that at the bigger gap G .

Figure 5(b) shows the situation at the wavelength of 768 nm. The zero reflection points are chosen to be at $G=310$, 340, and 550 nm. The region occupied by curve C becomes smaller when the wavelength approaches that of the coupled-SPP guided-mode resonance in SMG at 762 nm. The average sensitivities are $S_{G=310}=500^\circ/\text{RIU}$, $S_{G=340}=396^\circ/\text{RIU}$, and $S_{G=550}=136^\circ/\text{RIU}$. When the operating wavelength is shifted by only 2 nm toward λ_g (from 770 to 768 nm), the sensitivity is significantly increased. The sensitivity of point in curve B ($G=550$ nm) exhibits only a slight change over the operating wavelength. Results imply that when the operating wavelength is closer to λ_g , higher sensitivity can be achieved. Compared to other traditional SPPR-based sensors, the theoretical sensitivity is much higher than the $75^\circ/\text{RIU}$ of the single-grating SPPR-based sensor^[13] and the $191^\circ/\text{RIU}$ of the prism-coupling SPPR-based sensor with a smooth surface^[3].

The operating wavelength could not be infinitely close to λ_g ; otherwise, the operating region would become smaller and even disappear, and the signal-to-noise ratio would deteriorate. For example, in Fig. 5(b), the noise level should be smaller than 5% of the incident light; otherwise, we could not observe the exact valley of reflectance. With the structural parameters discussed here, curve C disappears in the angular reflection spectrum at the wavelength of 765 nm when $n_2=1.330$; therefore, the operating wavelength should be longer than 765 nm.

We propose an explanation about the high angular sensitivity achieved in the DMG structure. In general, for the SPPR-based sensor, high sensitivity is often related to a high Q -valued SPPR mode. However, in many cases, high sensitivity can be achieved when the system is under a critical balance over the refractive index variation, similar to the anti-crossing regime and the bending curves plotted in Figs. 2 and 4. When the gap G increases (decreases), the strength of the evanescent-field coupling effect decreases (increases) exponentially, while that of the F-P resonance effect exhibits a periodic oscillation. The two coupling effects then show comparable strength, especially at curve C. Considering that the refractive index variation inside the gap modifies both

the evanescent-field coupling and the F-P resonance effects, a strong response to the refractive index variation would be obtained if a way to break the balance between the two effects is determined, leading to high sensitivity. Adjusting the incident angle θ is one way, which can directly affect the evanescent-field coupling between the two SMGs, due to the modified phase difference among the non-zeroth diffracted evanescent modes while keeping the F-P resonance effect unchanged (as shown in curve A). This would result in the breaking of the critical balance between the two effects.

The abovementioned results show that in order to achieve higher sensitivity, a shorter wavelength λ and a smaller gap G are required. This seems conflicting because a shorter wavelength λ requires a larger gap G . Thus, G should have an optimal value. It is difficult to determine the exact balance point, but a proper operating point can be determined to achieve higher sensitivity.

In conclusion, we introduce an interesting reflection phenomenon in the DMG structure: when the gap between the two SMGs has a proper value, the curves of minimum reflection undergo an anti-crossing phenomenon and are slightly bent, which is caused by the interaction or competition between the evanescent-field coupling and the F-P resonance effects inside the gap. Due to the competition, a very small change in refractive index inside the gap of the DMG structure leads to a significant variation in the angular reflection spectra. Based on this, we theoretically present a reflex optical sensor with very high angular sensitivity. The calculated angular sensitivity is much higher than the theoretical sensitivity of traditional prism-coupling and grating-coupling SPPR-based sensors. By controlling the structural parameters, the operating wavelength could be flexible.

This work was supported by the National Natural Science Foundation of China (Nos. 10974102, 10874078, 11074116, and 10934003), the National Basic Research Program of China (No. 2006CB921805), and the Open Project of the State Key Laboratory of Functional Materials for Informatics.

References

1. J. Homola, S. S. Yee, and G. Gauglitz, *Sensors and Actuators B* **54**, 3 (1999).
2. J. M. Brockman, B. P. Nelson, and R. M. Corn, *Annu. Rev. Phys. Chem.* **51**, 41 (2000).
3. X. Fan, I. M. White, S. I. Shopova, H. Zhu, J. D. Suter, and Y. Sun, *Analytica Chimica Acta* **620**, 8 (2008).
4. K. Lin, Y. Lu, Z. Luo, R. Zheng, P. Wang, and H. Ming, *Chin. Opt. Lett.* **7**, 428 (2009).
5. J. Dostálek, J. Homola, and M. Miler, *Sensors and Actuators B* **107**, 154 (2005).
6. J. Homola, I. Koudela, and S. S. Yee, *Sensors and Actuators B* **54**, 16 (1999).
7. G. G. Nenninger, P. Tobisilka, J. Homola, and S. S. Yee, *Sensors and Actuators B* **74**, 145 (2001).
8. J. T. Hastings, J. Guo, P. D. Keathley, P. B. Kumares, Y. Wei, S. Law, and L. G. Bachas, *Opt. Express* **15**, 17661 (2007).
9. D. Sarid, *Phys. Rev. Lett.* **47**, 1927 (1981).
10. P. Adam, J. J. Dostálek, and J. Homola, *Sensors and Actuators B* **113**, 774 (2006).
11. J. Dostálek and J. Homola, *Sensors and Actuators B* **129**, 303 (2008).
12. A. J. Haes and R. P. Van Duyne, *J. Am. Chem. Soc.* **124**, 10596 (2002).
13. X. Yang and D. Liu, *Chin. Opt. Lett.* **5**, 563 (2007).
14. L. Pang, G. M. Hwang, B. Slutsky, and Y. Fainman, *Appl. Phys. Lett.* **91**, 123112 (2007).
15. Y. Li, J. Sun, L. Wang, P. Zhan, Z. Cao, and Z. Wang, *Appl. Phys. A* **92**, 291 (2008).
16. X. D. Hoa, A. G. Kirk, and M. Tabrizian, *Biosens. Bioelectron* **23**, 151 (2007).
17. H. Lu, Z. Cao, H. Li, and Q. Shen, *Appl. Phys. Lett.* **85**, 4579 (2004).
18. R. Slavík, J. Homola, J. Čtyroký, and E. Brynda, *Sensors and Actuators B* **74**, 106 (2001).
19. C. Cheng, J. Chen, Q.-Y. Wu, F.-F. Ren, J. Xu, Y.-X. Fan, and H.-T. Wang, *Appl. Phys. Lett.* **91**, 111111 (2007).
20. C. Cheng, J. Chen, D.-J. Shi, Q.-Y. Wu, F.-F. Ren, J. Xu, Y.-X. Fan, J. Ding, and H.-T. Wang, *Phys. Rev. B* **78**, 075406 (2008).
21. J. Xu, C. Cheng, Z. Zheng, J. Chen, Q. Bai, C. Liu, and H. Wang, *Chin. Opt. Lett.* **8**, 807 (2010).
22. J. A. Porto, F. J. Garcya-Vidal, and J. B. Pendry, *Phys. Rev. Lett.* **83**, 2845 (1999).
23. H. Zhao and D. Yuan, *Chin. Opt. Lett.* **8**, 1117 (2010).
24. J. T. Shen and P. M. Platzman, *Phys. Rev. B* **70**, 035101 (2004).
25. J. T. Shen, P. B. Catrysse, and S. Fan, *Phys. Rev. Lett.* **94**, 197401 (2005).